Experimental Validation of Reconstruction of Sound Source Radiation in an Underwater Half-Space Bounded by a Water-Air Interface

Zhimin Chen

College of Naval Architecture and Ocean Engineering, Naval University of Engineering, 717 Jiefang Road, Wuhan 430030, China.

Daren Zhou

East Lake Laboratory, 1101 Limiao Road, Wuhan 430203, China. E-mail: zhoudaren_svlab@163.com

Jingjun Lou

College of Naval Architecture and Ocean Engineering, Naval University of Engineering, 717 Jiefang Road, Wuhan 430030, China.

Min Peng

School of Artificial Intelligence, Wuhan Technology and Business University, 3 Huangjiahu West Road, Wuhan 430065, China.

Yongxiong Xiao

Zhejiang Lab, 1 Kechuang Avenue, Hangzhou 311121, China.

Xiangle Cheng and Zeyu Ru

Sound and Vibration Laboratory, College of Mechanical Engineering, Zhejiang University of Technology, 18 Chaowang Road, Hangzhou 310014, China.

(Received 20 September 2023; accepted 9 January 2024)

When a vibrating structure is located in a half-space bounded by a reflecting surface, the measured sound pressures are polluted by the reflection, so that they cannot show the actual sound radiation from the structure. The half-space spherical wave function expansion-based near-field acoustical holography approach is proposed to reconstruct the direct radiation from the sound source using the polluted sound pressures, which has been validated by numerical simulations. This paper deals with the experimental validation of this approach applied in an underwater half-space bounded by a water-air interface. The sound pressures measured in the half-space are used as the input data. The reconstructed sound pressures obtained are compared with benchmarks measured in a free space. The results indicate that the influences of the water-air interface reflection on the measured sound pressures can be greatly reduced in the entire frequency range investigated. The normalized relative reconstruction error introduced by the parameters of the hydrophone array and the water tank in the experiment is analyzed. The results of the experimental validation show that the proposed approach is promising for accurately measuring sound signals radiated from manned or unmanned vehicles or equipment underwater near a water-air interface.

1. INTRODUCTION

Near-field acoustical holography (NAH)[1–5] has been proven to be a powerful tool for reconstructing the three-dimensional sound field generated by a vibrating structure, using sound pressures measured by a sensor array in the near-field of the structure surface. Implementations of NAH generally require that the sensor array be placed in a source-free region, because they utilize the free-space Green's functions to relate the radiated sound pressures at different field points. Hence, when the measured sound pressures are polluted by reflections from any surfaces existing near the source, reconstruction of the sound field that is radiated directly from the source cannot be realized via these NAH methods.[6] However, a bounded space with reflecting surfaces underwater is more commonly encountered than a free space in practice.

In a half-space bounded by a reflecting surface,[6] the sound field has to be modeled using half-space Green's functions[7] satisfying the Helmholtz equation along with the boundary condition. By replacing the free-space Green's functions with the half-space Green's functions in NAH formulations, reconstruction of the sound field in the half-space can be realized.[8] The Fourier acoustics-based approach[9] was employed to reconstruct the sound field radiated directly from a planar source facing a parallel impedance surface. In addition, an experimental validation in an air medium was conducted. The inverse boundary element method-based approach[6] was utilized to reconstruct the acoustic quantities on the source surface located in a half-space bounded by a rigid surface; and numerical validations for a spherical source and a finite cylindrical

source in an air medium were demonstrated. The equivalent source method-based approach[10,11] was applied to reconstruct the acoustic quantities on the source surface located in a half-space bounded by an impedance surface, and the reconstruction of both the stationary and transient sound fields was validated by numerical simulations and experiments conducted in an air medium. The half-space spherical wave function expansion-based approach[8,12,13] was proposed to reconstruct the sound field radiated directly from a source located near an impedance surface, and the numerical and experimental validations conducted in an air medium were demonstrated. This method was also recently applied to a half-space bounded by a pressure-release surface, which was validated by numerical simulations.[14]

The aforementioned half-space sound field reconstruction approaches were either numerically or experimentally validated in an air medium. However, there is so far little literature focusing on the experimental validation of these approaches applied in an underwater half-space, although an underwater half-space is a commonly encountered environment in practice where correctly acquiring the underwater sound radiation from manned or unmanned underwater vehicles matters.[15,16] This study aims to experimentally validate the half-space spherical wave function expansion-based approach in an underwater medium in the presence of a water-air interface. Since the water-air interface can be treated as a natural pressure-release boundary,[17] the sound pressures radiated directly from the source in water can be reconstructed using the formulations proposed in References.[14] In this study, the experimental setup is discussed in detail first. Then, the reconstructed sound pressures at the measurement points are compared with the benchmarks measured in an anechoic water tank to validate the proposed approach. The impacts of the parameters on the reconstruction accuracy are examined.

2. MATHEMATICAL MODELING

The mathematical modeling of the half-space spherical wave function expansion-based approach applied to a half-space bounded by a pressure-release surface has been proposed in References,[14] and is briefly presented here. As shown in Fig. 1, a global coordinate system with the *x*-*y* plane set on the boundary of the water-air interface is defined such that the global coordinates of the geometrical center of the sound source structure O_1 and the center of its mirror image O_2 about the interface are given by $\mathbf{x}_{O_1} = (0, 0, -h_\mathrm{s})$ and $\mathbf{x}_{O_2} = (0, 0, h_\mathrm{s})$, respectively. A hologram surface, which holds hydrophones at M points near the surface of the source, is used to measure the sound pressures in the half-space. The sound pressures radiated directly from the source can be correlated to the half-space sound pressures via a transfer matrix, as[14]:

$$\{p^{\mathrm{rec}}(\mathbf{x}_s;\omega)\}_{S\times 1} = [G_p(\mathbf{x}_s|\,\mathbf{x}_m;\omega)]_{S\times M}\{p^{\mathrm{meas}}_{\mathrm{half}}(\mathbf{x}_m;\omega)\}_{M\times 1}; \quad (1)$$

where $\{p^{\mathrm{rec}}(\mathbf{x}_s;\omega)\}_{S\times 1}$ is a column vector of the reconstructed sound pressures, radiated directly from the source; the vectors $\mathbf{x}_s$, $s = 1$ to S, denote the coordinates of the reconstruction points; ω is the angular frequency; $\{p^{\mathrm{meas}}_{\mathrm{half}}(\mathbf{x}_m;\omega)\}_{M\times 1}$ is a column vector of the sound pressures measured in the half-space; the vectors $\mathbf{x}_m$, $m = 1$ to M, denote the coordinates of hydrophones; and

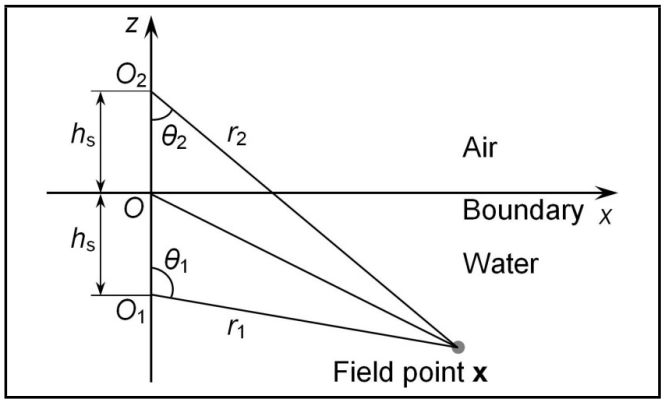

Figure 1. Geometry of a half-space bounded by a water-air interface, where O_1 is the geometrical center of a sound source structure in water and O_2 is the corresponding mirror image about the interface.

$[G_p(\mathbf{x}_s|\,\mathbf{x}_m;\omega)]_{S\times M}$ represents the transfer matrix that correlates the sound pressures measured in the half-space at $\mathbf{x}_m$ to the sound pressures radiated directly from the source at $\mathbf{x}_s$.

The transfer matrix $[G_p(\mathbf{x}_s|\,\mathbf{x}_m;\omega)]_{S\times M}$ is given by:

$$[G_p(\mathbf{x}_s|\,\mathbf{x}_m;\omega)]_{S\times M} = [\psi(\mathbf{x}_s,\mathbf{x}_{O_1};\omega)]_{S\times J}[\psi_{\mathrm{half}}(\mathbf{x}_m;\omega)]^{\dagger}_{J\times M}; \quad (2)$$

where $[\psi(\mathbf{x}_s,\mathbf{x}_{O_1};\omega)]_{S\times J}$ is a matrix of free-space spherical wave functions $\psi_j(\mathbf{x}_s,\mathbf{x}_{O_1};\omega)$; $[\psi_{\mathrm{half}}(\mathbf{x}_m;\omega)]_{M\times J}$ is a matrix of half-space spherical wave functions; j is the index of the expansion terms, ranging from 1 to J; and the superscript † denotes the pseudo-inverse of a matrix.

The water-air interface is physically a pressure-release boundary of the underwater half-space. The half-space spherical wave functions $\psi_{j\ \mathrm{half}}(\mathbf{x};\omega)$ satisfying the pressure-release boundary condition are given by:[14]

$$\psi_{j\ \mathrm{half}}(\mathbf{x};\omega) = \psi_j(\mathbf{x},\mathbf{x}_{O_1};\omega) + (-1)\cdot\psi_j(\mathbf{x},\mathbf{x}_{O_2};\omega); \quad (3)$$

where $\psi_j(\mathbf{x},\mathbf{x}_{O_1};\omega)$ and $\psi_j(\mathbf{x},\mathbf{x}_{O_2};\omega)$ are the spherical wave functions in free space, representing[14] the sound radiation from a multipole or a group of multipoles in a water medium centered at $\mathbf{x}_{O_1}$, and the corresponding mirror image sources centered at $\mathbf{x}_{O_2}$, respectively. They are the solutions to the Helmholtz equation, expressible in spherical coordinates as:

$$\psi_j(\mathbf{x};\omega) \equiv \psi_{nl}(r,\theta,\phi;\omega) = h^{(1)}_n(kr)\,Y^l_n(\theta,\phi); \quad (4)$$

where $h^{(1)}_n(kr)$ are the spherical Hankel functions of the first kind, and $Y^l_n(\theta,\phi)$ are the spherical harmonics. The indices n, l and j in Eq. (4) are related by $j = n^2 + n + l + 1$, with n ranging from 0 to N and l from $-n$ to n.

The two local coordinate systems with the origins O_1 and O_2 in Fig. 1 are established by translations of the global coordinate system with the origin O. The local coordinates of a field point $\mathbf{x}_1 \equiv (r_1,\theta_1,\phi_1)$ with the origin O_1 and $\mathbf{x}_2 \equiv (r_2,\theta_2,\phi_2)$ with the origin O_2 are related to the global coordinates $\mathbf{x}$ by:

$$\mathbf{x}_1 = \mathbf{x} + h_\mathrm{s}\mathbf{e}_z, \quad \mathbf{x}_2 = \mathbf{x} - h_\mathrm{s}\mathbf{e}_z; \quad (5)$$

where $\mathbf{e}_z$ is the unit vector in the z direction, i.e., a normal vector to the water-air interface.

The accuracy in reconstruction of the direct radiation from the sound source, $\{p^{\mathrm{rec}}(\mathbf{x}_s;\omega)\}_{S\times 1}$, depends on the number

of expansion terms J in Eq. (2). The same procedure of determining an optimal number J_{opt} of expansion terms has been adopted as in related recent publications.[14] In addition, because the transfer matrix $[G_p(\mathbf{x}_s|\mathbf{x}_m;\omega)]_{S\times M}$ defined in Eq. (2) is generally ill-conditioned, a modified Tikhonov regularization,[1,6] implemented through singular value decomposition, is employed. The regularization parameter is determined by the generalized cross-validation procedure.[1,6]

3. EXPERIMENTAL VALIDATION

3.1. Setup of the Experiment

The experiment was carried out in a cubic water tank, its four vertical walls and bottom floor covered with sound-absorptive materials. The top surface of the volume of water in the tank can be either opened to air or fully closed by covering it piece-wise with sound-absorptive materials. When the top surface is opened to air, a half-space bounded by a water-air interface is constructed, and the measurements of half-space sound pressures can be conducted. When the top surface is covered by sound-absorptive materials, an anechoic space is constructed, and the measurements of benchmarks of the direct radiation from the sound source can be conducted. The internal dimensions of the water tank covered with sound-absorptive materials are 2.51 meters long, 2.07 meters wide and 2.2 meters high. The sound-absorptive materials consist of wedge-shaped elements, the longest wavelength of sound can be absorbed and is positively related to the length of the wedge. In this experiment, the absorption coefficient of the walls, bottom floor and top covering is 0.9 or higher, and the cut-off low frequency is 5 kHz.

The setup of the sound source and hydrophone array inside the water tank is shown in Fig. 2. A sound source and a hydrophone array which were readily available in the Sound and Vibration Laboratory were used in the experiment. The sound source was a cylindrical transducer with a diameter of 0.185 m and a length of 0.320 m, which radiated sound in the interior space of the water tank. The planar hydrophone array, with an aperture of 0.375 m $\times$ 0.375 m, was used to form a hologram surface for measuring sound pressures. There were $7\times 7=49$ hydrophones uniformly distributed on the array, and the spacing between hydrophones was 0.0625 m. A hologram surface that did not conform to the surface of the sound source structure was employed not only to examine the robustness of the approach, but also for reasons of implementation feasibility and cost-effectiveness of the proposed approach in potential engineering applications.

3.2. Implementation of the Experiment

A schematic of measuring the sound pressures inside the water tank is shown in Fig. 3. A global coordinate system was set such that the water-air interface was in the *x*-*y* plane and the geometric center O_1 of the sound source structure was at $\mathbf{x}_{O_1}=(0,0,-h_{\mathrm{s}})$, where $h_{\mathrm{s}}=0.44$ m was the distance between O_1 and the water-air interface. The longitudinal axis of the source structure was parallel to the water-air interface, as well as to the hologram surface, which was perpendicular to the water-air interface. The geometric center of the hologram surface was placed at $\mathbf{x}_{\mathrm{ar}}=(0,-d_{\mathrm{s}},-h_{\mathrm{s}})$, where $d_{\mathrm{s}}=0.170$ m was the distance between O_1 and the hologram surface. The speed of sound was $c=1500$ m/s.

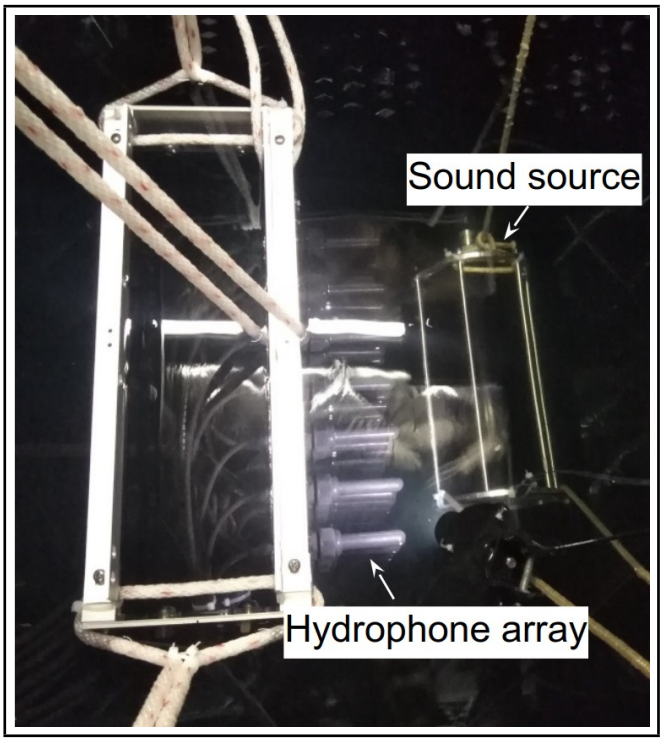

Figure 2. Setup of the sound source and the hydrophone array inside the water tank.

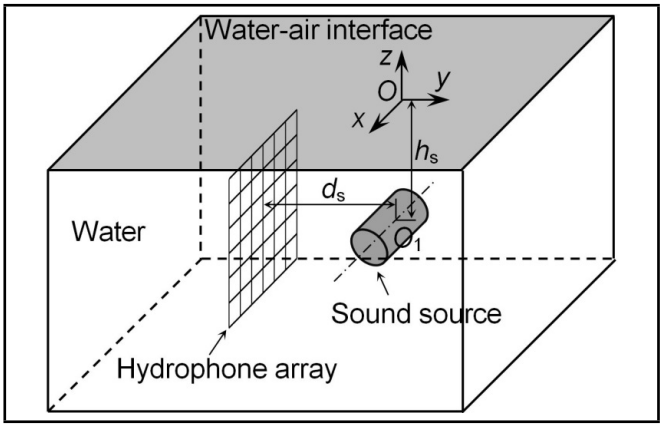

Figure 3. Schematic of measuring sound pressures inside the water tank.

Both the measurements of the sound pressures in the half-space (the half-space sound pressures) and in the anechoic space (the benchmarks) were taken in a frequency range from 4 kHz to 8 kHz, with 1 kHz increments, corresponding to 3 to 6 measurement points within a wavelength. The half-space sound pressures were taken as the input data, and the sound pressures at the measurement points radiated directly from the source were reconstructed. To quantify the reconstruction accuracy in the experimental validation, normalized relative reconstruction error ε is defined as:

$$\varepsilon=\frac{\left\|\left\{p^{\mathrm{rec}}(\mathbf{x}_m;\omega)\right\}_{M\times 1}-\left\{p^{\mathrm{ben}}(\mathbf{x}_m;\omega)\right\}_{M\times 1}\right\|_2}{\left\|\left\{p^{\mathrm{ben}}(\mathbf{x}_m;\omega)\right\}_{M\times 1}\right\|_2}\times 100\%; \tag{6}$$

where $\left\{p^{\mathrm{ben}}(\mathbf{x}_m;\omega)\right\}_{M\times 1}$ is a column vector of the benchmarks and $\|\cdot\|_2$ denotes the 2-norm of a vector. Normalized

relative measurement error E is also defined, as:

$$E = \frac{\left\| \{p_{\text{half}}^{\text{meas}}(\mathbf{x}_m;\omega)\}_{M\times 1} - \{p^{\text{ben}}(\mathbf{x}_m;\omega)\}_{M\times 1} \right\|_2}{\left\| \{p^{\text{ben}}(\mathbf{x}_m;\omega)\}_{M\times 1} \right\|_2} \times 100\%. \tag{7}$$

Measurement error E is defined to quantify the influences of the boundary reflection on the measured sound pressures without applying the proposed approach.

3.3. Results and Discussion

The experimental results for frequencies 4–8 kHz are demonstrated with two-dimensional holographic images, as shown in Fig. 4. The measured half-space sound pressures, the reconstructed sound pressures obtained by using the proposed approach and the benchmarks are shown in the left, middle and right columns, respectively. The images in each row correspond to a single frequency. Each of the two-dimensional images presents the amplitude of the sound pressure distribution in an area of 0.250 m $\times$ 0.250 m, which is the area of the hologram surface covered by the inner 5×5 hydrophones.

The influence of the water-air interface reflection on the underwater sound field can be qualitatively observed by comparing the images of half-space sound pressures in the left column and the benchmarks in the right column. For instance, take the case where the frequency $f = 5$ kHz, as shown in Figs. 4(d), 4(e) and 4(f). It is found from the image of the benchmarks that the amplitude of the sound pressure reaches its maximum at the center area and then decays as the observation point moves from the center towards the four corners. The contour shapes of the benchmark image indicate that the amplitudes of the sound pressures near the middle section of the source are larger than those near the two ends of the source.

However, the sound reflection from the water-air interface drastically disturbs the pressure distribution in the underwater half-space. As shown in Fig. 4(d), the amplitude of the half-space sound pressure reaches its maximum at a point shifted from the center towards the bottom of the hologram surface. It is also found that the maximum value of the half-space sound pressure differs from that of the benchmark. Observing the contour shapes, it is found that there are multiple extreme points rather than one extreme point. Hence, the sound pressures measured in the half-space cannot be taken as the values radiated directly from the sound source in the underwater field. An approach such as the proposed one has to be employed to overcome the reflection from the water-air interface to get more accurate values of sound radiation from the source.

All the images of the reconstructed sound pressures obtained by using the proposed approach are shown in the middle column of Fig. 4. By comparing the three images obtained at each frequency, it is obvious that the image of the reconstructed values is more agreeable with the image of benchmarks than the image of half-space values. The results indicate that the influences caused by the water-air interface reflection on the measured sound pressures have been reduced significantly by using the proposed approach.

The normalized relative errors E and ε, defined in Eqs. (6) and (7), were calculated to quantitatively evaluate the reconstruction accuracy of the proposed approach. The curves of E and ε versus frequency are shown in Fig. 5. It is found that the normalized relative reconstruction error ε is much lower than the value of straightforward measurement error E at every frequency. It reveals that the reconstruction errors ε obtained at most frequencies are lower than 20%, and even lower than 10% at some frequencies. These data intuitively indicate that the reconstructed sound pressures are closer to the benchmarks radiated directly from the sound source than the measured half-space sound pressures are, and that the reconstructed values can more accurately reflect the sound pressure field radiated directly from the source.

Note that there are limitations of the frequency range in the experiment imposed by the equipment. The low-frequency bound is limited by the physical size of the water tank and the ability of the absorptive materials on the interior boundary of the tank to absorb sound waves with longer wavelengths. The high-frequency bound is constrained by the spacing of the hydrophones in the array, which is therefore unable to collect the higher-wavenumber components of the sound field. These limitations are reflected in the reconstruction error ε curve, in that the errors obtained at 4 kHz, 7 kHz and 8 kHz are larger than those obtained at 5 kHz and 6 kHz. Hence, when dealing with sound fields with a frequency higher than 8 kHz, more hydrophones should be used in order to obtain acceptable reconstruction accuracy.

Moreover, the planar hydrophone array employed in the experiment, not conformal to the surface of the cylindrical sound source also contributes to the normalized relative reconstruction error ε. The hydrophones at the edges of the hologram surface receive lower levels of direct source radiation than the hydrophones near the center of the hologram surface. As the frequency increases, the sound field on the hologram surface tends to concentrate near the center of the surface. The sound pressures measured at the edges of the hologram surface will contain less contribution from the source but more contribution from the boundary reflection, which leads to a reduced sound power ratio of the direct radiation relative to the boundary reflection at the measurement points. In fact, this sound power ratio[14] is an important parameter affecting the accuracy in reconstruction of the directly radiated field form the source using the half-space spherical wave function expansion-based approach. Generally, the larger the ratio is, the higher the accuracy tends to be.[14] Consequently, the reconstruction accuracy deteriorates with the increasing frequency. This deterioration can be remedied by using a cylindrical hologram surface which is conformal to the source surface.

4. CONCLUSIONS

The experimental validation of the half-space spherical wave function expansion-based approach for reconstruction of the sound source radiation in an underwater half-space bounded by a water-air interface is presented. The experiment was carried out in a cubic water tank, which could be configured as a semi-anechoic underwater space bounded by a water-air interface or as a fully anechoic space. Both the sound pressures directly measured in the half-space and the reconstructed sound pressures obtained by using the proposed approach were compared with benchmarks measured in the anechoic space. The results showed that the reconstructed sound pressures were much closer to the benchmarks than the directly measured half-space sound pressures were, indicating that the influences caused by the water-air interface reflection on the measured sound pressures were reduced significantly by using the proposed approach. The normalized relative reconstruction error introduced by the parameters of the hydrophone array and the water tank in the experiment was also analyzed. This

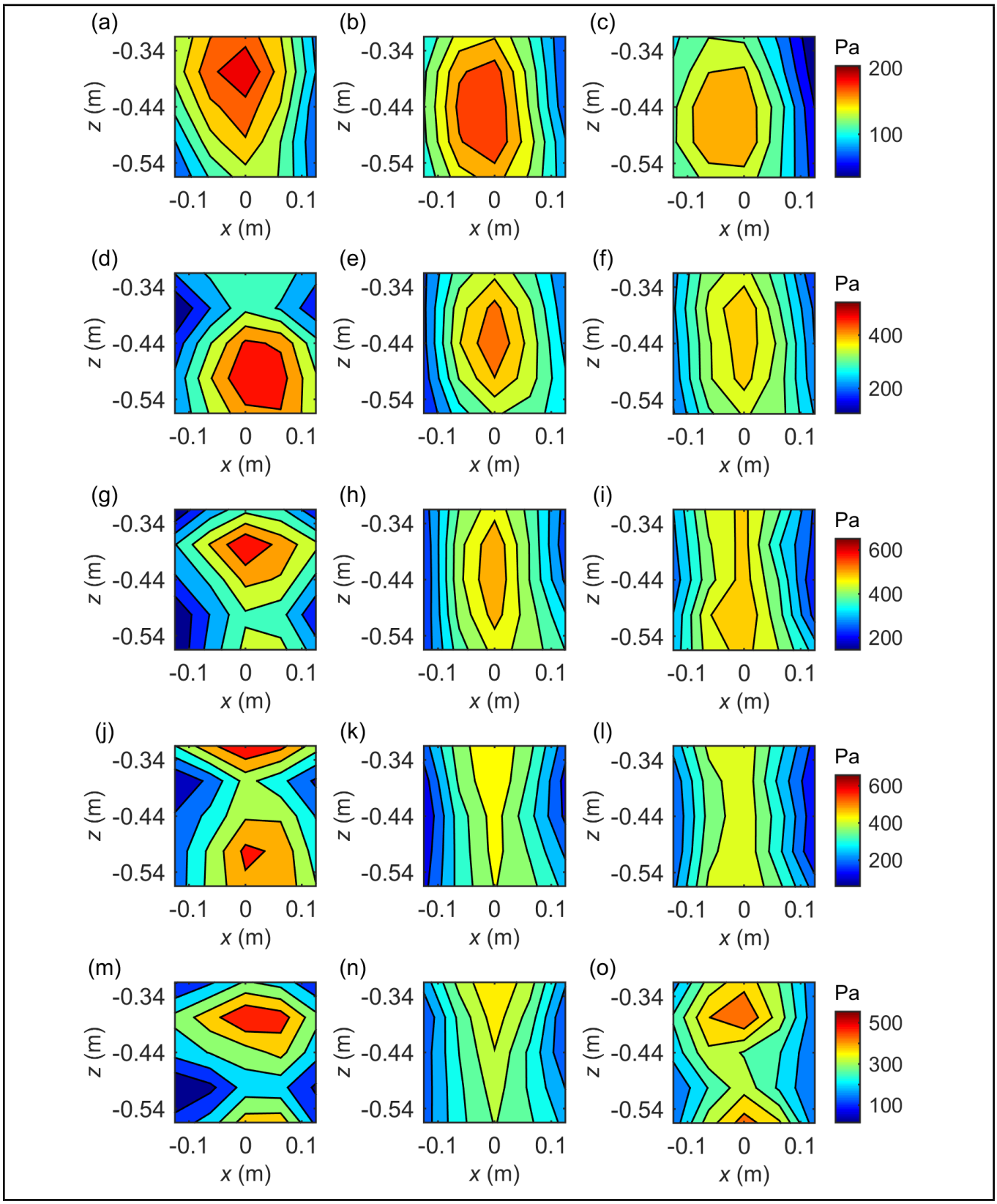

Figure 4. Two-dimensional holographic images of the sound pressure amplitudes for frequencies $f = 4$ kHz–8 kHz arranged from the top to the bottom by rows. The left column shows the half-space sound pressures, the middle column the reconstructed sound pressures and the right column the benchmarks.

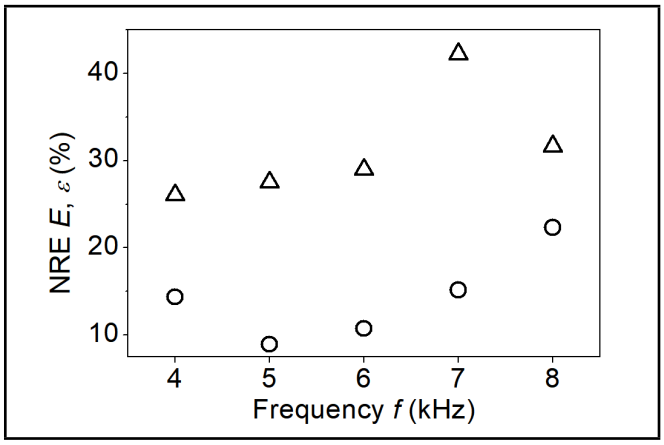

Figure 5. Normalized relative measurement error E (△) and reconstruction error ε (○) calculated at different frequencies.

experimental validation proved that the proposed approach is promising for the accurate measurement of sound signals generated by a variety of manned or unmanned vehicles or equipment underwater near a water-air interface.

ACKNOWLEDGEMENTS

This research was supported by the Natural Science Foundation of China 52205133, 51975525, 52005443, 52105128; the "One Belt One Road" program through Zhejiang Province and the Zhejiang University of Technology-Institute of Applied Physics, Russian Academy of Sciences Joint Research Laboratory of Innovative Technology of Sound and Vibration 2018C04018; and the Natural Science Foundation of Zhejiang Province LQ21E050016.

REFERENCES

[1] Wu, S. F. Methods for reconstructing acoustic quantities based on acoustic pressure measurements, *J. Acoust. Soc. Am.*, **124** (5), 2680–2697, (2008). https://doi.org/10.1121/1.2977731

[2] Zhang, M. Y., Hu, D. Y., Yang, C., Shi, W. and Liao, A. H. An improvement of the generalized discrete Fourier series based patch near-field acoustical holography, *Appl. Acoust.*, **173**, 107711, (2021). https://doi.org/10.1016/j.apacoust.2020.107711

[3] Luo, Z. W., Comesana, D. F., Zheng, C. J. and Bi, C. X. Near-field acoustic holography with three-dimensional scanning measurements, *J. Sound Vib.*, **439**, 43-55, (2019). https://doi.org/10.1016/j.jsv.2018.09.049

[4] Wu, S. F. *The Helmholtz Equation Least-Squares Method*, Springer, New York, (2015). https://doi.org/10.1007/978-1-4939-1640-5

[5] Jiang, L., Xiao, Y., Zou, G. and Ih, J. -G. Optimal sensor positioning for the sparse measurement in the acoustic reconstruction of a large source, *IEEE Trans. Instrum. Meas.*, **72**, 6502513, (2023). https://doi.org/10.1109/TIM.2023.3267533

[6] Xiang, Z. and Wu, S. F. Reconstruction of vibroacoustic fields in half-space by using hybrid near-field acoustical holography, *J. Acoust. Soc. Am.*, **117** (2), 555-565, (2005). https://doi.org/10.1121/1.1847994

[7] Okoyenta, A. R., Wu, H., Liu, X. and Jiang, W. A short survey on green's function for acoustic problems, *J. Theor. Comput. Acous.*, **28** (2), 1950025, (2020). https://doi.org/10.1142/S2591728519500257

[8] Zhou, D., Lu, H., McFarland, D. M. and Xiao, Y. Reconstruction of acoustic radiation of a vibrating structure located in a half-space bounded by a passive surface with finite acoustic impedance, *J. Theor. Comput. Acous.*, **28** (4), 2050019, (2020). https://doi.org/10.1142/S259172852050019X

[9] Zea, E. and Arteaga, I. L. Sound field separation for planar sources facing a parallel reflector, *Appl. Acoust.*, **149**, 181-191, (2019). https://doi.org/10.1016/j.apacoust.2019.01.030

[10] Bi, C. X., Jing, W. Q., Zhang, Y. B. and Lin, W. L. Reconstruction of the sound field above a reflecting plane using the equivalent source method, *J. Sound Vib.*, **386**, 149-162, (2017). https://doi.org/10.1016/j.jsv.2016.09.029

[11] Pan, S. W., Jiang, W. K., Zhang, H. B. and Xiang, S. Modeling transient sound propagation over an absorbing plane by a half-space interpolated time-domain equivalent source method, *J. Acoust. Soc. Am.*, **136** (4), 1744-1755, (2014). https://doi.org/10.1121/1.4895705

[12] Zhou, D., Xiao, Y. and Lu, H. Reconstruction of the direct radiation from a source using the expansion in half-space spherical wave functions, *Acta Acust.*, **46** (3), 321-334, (2021). (in Chinese) https://doi.org/10.15949/j.cnki.0371-0025.2021.03.001

[13] Zhou, D., Lu, H., Cheng, X. and McFarland, D. M. Reconstruction of half-space boundary impedance and sound source direct radiation based on reflection coefficient estimation, *Acta Phys. Sin.*, **71** (12), 124301, (2022). (in Chinese) https://doi.org/10.7498/aps.71.20211924

[14] Chen, Z., Zhou, D. and Lou, J. Reconstruction of the acoustic field radiated directly from a vibrating structure located near a pressure-release boundary, *Int. J. Acoust. Vib.*, **27** (4), 354-360, (2022). https://doi.org/10.20855/ijav.2022.27.41886

[15] *Underwater acoustics – Quantities and procedures for description and measurement of underwater sound from ships – Part 1: Requirements for precision measurements in deep water used for comparison purposes*, International Standard ISO 17208-1: 2016, International Organization for Standardization, Geneva, Switzerland, (2016).

[16] Hawkes, M. and Nehorai, A. Acoustic vector-sensor processing in the presence of a reflecting boundary, *IEEE Trans. Signal Process.*, **48** (11), 2981-2993, (2000). https://doi.org/10.1109/78.875455

[17] Blackstock, D. T. *Fundamentals of Physical Acoustics*, Wiley, New York, (2000). https://doi.org/10.1121/1.1354982